ACS Catalysis

Research Article

pubs.acs.org/acscatalysis

Molecular Photoelectrocatalysts for Visible Light-Driven Hydrogen Evolution from Neutral Water

Catherine L. Pitman and Alexander J. M. Miller*

Department of Chemistry, University of North Carolina at Chapel Hill, Chapel Hill, North Carolina 27599-3290, United States

Supporting Information

ABSTRACT: A light-activated hydrogen evolution electrocatalyst is reported. Hydrogen evolves near the thermodynamic potential when aqueous solutions of the iridium chloride complex [Cp*Ir(bpy)(Cl)][Cl] (**1**, bpy = 2,2′-bipyridine) are illuminated by visible light. In the dark, no electrocatalytic activity is observed. This unique hydrogen evolution mechanism is made possible because a single transition metal complex is the active light absorber and active electrocatalyst. Optimization by tuning the electronic structure of the catalyst and varying reaction conditions resulted in H_2 evolution with faster rates, even at milder applied potentials ($k_{obs} \sim 0.1\ s^{-1}$ at 100 mV electrochemical overpotential).

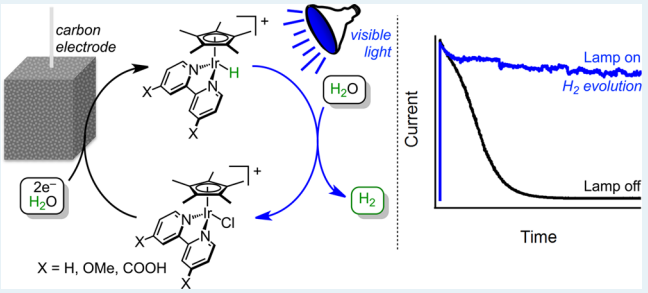

KEYWORDS: *hydrogen evolution, photoelectrocatalysis, iridium, hydride, photocatalysis, electrocatalysis*

INTRODUCTION

Light-promoted evolution of hydrogen from water has long been recognized as an attractive route to solar fuels. Diverse strategies for hydrogen evolution have emerged, from simple, single-component systems for photocatalytic acid-splitting to modular, multicomponent approaches featuring separate light absorber and catalyst components.[1] In multicomponent schemes, the catalyst is often identified and optimized using electrochemical methods before integration with a light absorber.[2] The multicomponent photoredox approach has seen widespread success in systems utilizing a molecular chromophore (e.g., $Ru(bpy)_3^{2+}$), a catalyst (e.g., Co diglyoximes), and a sacrificial reductant.[3] A light absorbing material (e.g., Si or small-band-gap semiconductors) can also be employed in such systems, leading to heterogeneous photoelectrochemical cells.[4]

We envisioned an alternative photoelectrochemical approach, in which H_2 evolution is facilitated by a *single* molecule acting *both* as light absorber *and* electrocatalyst. A related strategy involves using the coordinatively saturated chromophore $Ru(bpy)_3^{2+}$ to perform a photochemical redox reaction before electrochemical regeneration at an electrode, but this strategy has not been applied to the synthesis of a chemical fuel, as in hydrogen evolution catalysis.[5] We report here that [Cp*Ir(bpy)(Cl)][Cl] (**1**) integrates light absorption and electrocatalysis in a single molecular framework. Aqueous solutions of **1** evolve negligible amounts of H_2 in the dark at pH 7, but illumination with visible light initiates sustained photoelectrocatalytic H_2 evolution with minimal applied potential (Scheme 1). Electron transfer occurs in the dark, whereas H_2 release is light-triggered, consistent with previously observed reactivity pertaining to the photochemical water−gas shift reaction.[6] Unlike the water−gas shift and other multicomponent hydrogen evolution strategies, no sacrificial reagent is required. Tuning the electronic nature of the ligand affords photoelectrocatalysts with good activity near the thermodynamic potential for H_2 evolution.

Scheme 1. Photoelectrochemical Water Reduction Conditions

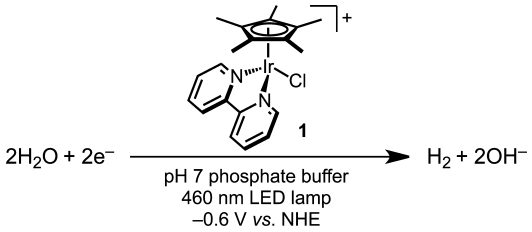

RESULTS AND DISCUSSION

Sustained Photoelectrocatalytic Hydrogen Evolution.

A molecular photoelectrocatalyst must be capable of electrochemical hydride formation and photochemical H_2 release. Detailed electrocatalytic studies of **1** in aqueous solution are lacking,[7] but H_2 evolution electrocatalysis in acetonitrile has been reported, albeit at very negative potentials (−1.6 V vs Ag/Ag^+).[8] Considering this precedent, electrochemical studies in aqueous solution were undertaken, in the dark and under visible light illumination.

Received: April 3, 2014
Revised: June 11, 2014
Published: July 7, 2014

   dx.doi.org/10.1021/cs500441f | ACS Catal. 2014, 4, 2727−2733

Water-soluble chloride complex **1** was prepared according to the previously reported procedure,[9] and cyclic voltammetry (CV) was performed as an initial probe for photoelectrocatalytic activity. In pH 7 phosphate buffer (0.1 M), protected from light, chloride complex **1** exhibited an irreversible reduction at −0.61 V on a glassy carbon working electrode (Figure 1; all

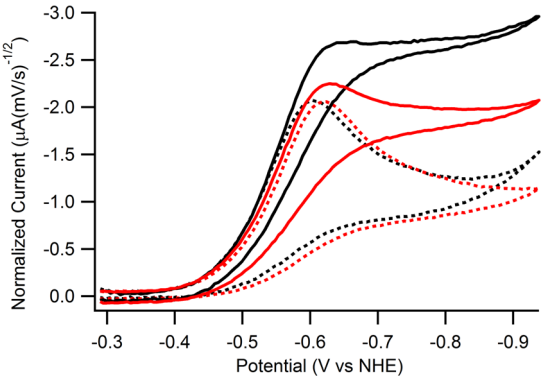

Figure 1. CV of 1 mM **1** in 0.1 M phosphate buffer (pH 7) at 5 mV·s^{-1} under illumination (solid black) and in the dark (dashed black) and at 10 mV·s^{-1} under illumination (solid red) and in the dark (dashed red). Glassy carbon working electrode (3 mm disc), Pt wire counter electrode, Ag/AgCl (3 M NaCl) reference electrode, 460 nm LED lamp. Current is scan-rate-normalized: normalized current of diffusion-controlled processes is constant with changing scan rate whereas normalized current of catalytic waves increases as the scan rate decreases.

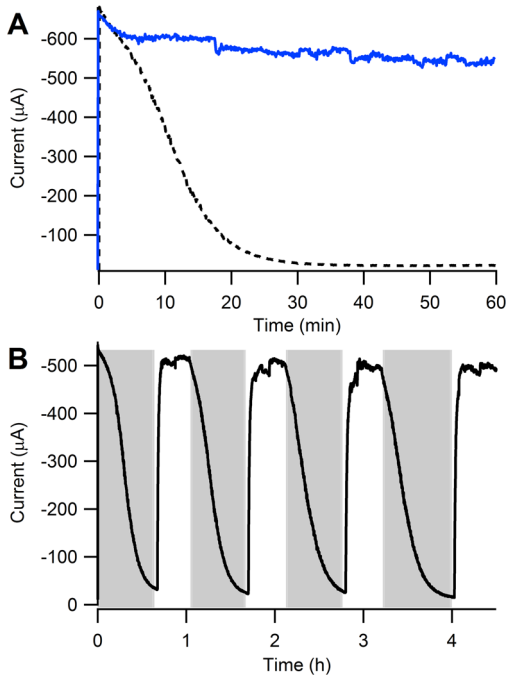

Figure 2. (A) CPE at −1 V vs NHE of 1 mM **1** in 0.1 M phosphate buffer (pH 7) in the dark (dashed black) and under 460 nm light (solid blue). (B) CPE at −0.9 V vs NHE of 1 mM **1** in 0.1 M phosphate buffer (pH 7) with light off (gray) and on (white). Reticulated vitreous carbon working electrode, Pt wire counter electrode, Ag/AgCl (3 M NaCl) reference electrode.

potentials reported vs NHE unless otherwise noted). At scan rates of 25 mV·s^{-1} and faster, no current enhancement was observed upon illumination with a 460 nm LED lamp. At scan rates slower than 25 mV·s^{-1}, however, illumination produced clear increases in current (Figure 1). At such slow scan rates, convection can interfere with interpretation,[10] but the current enhancement is characteristic of catalysis.

Encouraged by the current response to light in CV experiments, controlled potential electrolysis (CPE) was carried out to provide further support for photoelectrocatalysis. In CPE experiments with the potential held at −1 V vs NHE, a 1 mM solution of **1** in pH 7 phosphate buffer was irradiated at 460 nm. Sustained photocurrent around −600 μA was achieved over the course of the 1 h experiment (Figure 2A), and bubbles evolved from solution and accumulated on the electrodes. When protected from light, the high initial current rapidly diminished to below −25 μA, consistent with a stoichiometric electrochemical process (Figure 2A). The CPE experiments confirm that although chloride **1** is an ineffective electrocatalyst in the dark, photolysis induces electrocatalytic activity (Scheme 1). Visible light enhanced catalytic currents by a factor of roughly 25 after 60 min at −1 V, suggesting efficient and sustained photoelectrocatalysis.

The influence of light was further established by applying a shutter to CPE experiments (Figure 2B). In the dark, high levels of current are initially passed before rapidly decaying, consistent with complete electrochemical reduction of all **1** in solution. In the light, the current quickly rises and remains steady as photoelectrocatalytic H_2 evolution initiates. Applying a shutter halts catalysis, and the current immediately begins to drop. The large amount of charge passed after shuttering implies that hydride **2**, which cannot be further reduced at the potential applied, is not the dominant species in the bulk solution during catalysis. The low proportion of hydride **2** in solution suggests that the photochemical steps are not limiting the reaction in this cell configuration. As a control reaction, the same experiment was performed in the absence of catalyst: no difference in current was observed when a cell containing only aqueous phosphate buffer was toggled between dark and light conditions.

The faradic efficiency of photoelectrocatalysis was quantified by monitoring the solution pH change in situ during photoelectrolysis. If H_2 is produced according to Scheme 1, proton consumption will lead to a pH increase. Faradic efficiency was obtained by relating the measured pH change to the expected pH change if every two electrons produced H_2.[11] A weakly buffered solution (50 mM phosphate, initial pH 7.8) was irradiated while applying a potential of −0.9 V, and the pH was measured periodically. The pH increased as expected, with 100% faradic efficiency recorded at early times before a slight decrease to ∼90% as the experiment proceeded and the pH increased (Supporting Information (SI) Figure S2).

The photon-to-hydrogen efficiency is also of great interest in photoelectrocatalytic processes. This efficiency can be measured in a number of ways; the present system, in which the specific concentration of photoactive species at any given time is unknown, was assessed by "external quantum efficiency" (EQE = (moles H_2 produced)/(moles incident photons)). The moles of incident photons in the area of the electrode were measured using a Si photodiode. On the basis of the current passed and the faradic efficiency, EQE = 10(5)% in three separate controlled potential electrolysis experiments. This value is similar to a previous molecular photoelectrochemical cell based on photoredox quenching[5b] and similar to the H_2 quantum yield in photochemical water−gas shift reactions involving **2**.[6c] It is expected that the EQE value obtained here

dx.doi.org/10.1021/cs500441f | ACS Catal. 2014, 4, 2727−2733

will be sensitive to a variety of factors, such as the light source, cell geometry, electrode surface area (variations in which we believe to be responsible for the relatively large uncertainty in our value), catalyst concentration, and applied potential. The EQE is useful for practical catalytic applications; the mechanistically more insightful quantum yield, which measures the efficiency of H_2 evolution based on the number of photons actually *absorbed* by hydride **2**, will be assessed in future studies.

In prolonged photoelectrocatalysis experiments, photocurrent was relatively stable until the buffer was exhausted after 5.5 h. The total catalyst turnover number (TON) for H_2 production in this extended experiment was 16.5 (TON ∼ 3.9 in a typical 1 h experiment).[12] Photoelectrocatalytic activity was restored upon addition of acid, but steadily diminishing current over the course of 48 h suggests some catalyst degradation (SI Figure S3). In dark electrolyses under the same conditions, no H_2 was detected by GC. Similarly, when phosphate solutions (no catalyst) were subjected to photoelectrolysis, minimal charge passed (−0.17 C without catalyst, −1.23 C with catalyst), and the pH did not change.

Separating the Electrochemical and Photochemical Steps. To establish that catalyst **1** was responsible for both the photochemical and electrochemical processes, they were studied independently. First, the electrochemical properties of **1** were probed in the absence of light. As described above, CV of **1** in pH 7 phosphate buffer (0.1 M) displays an irreversible reduction around −0.61 V that appears to be composed of multiple peaks. In contrast, solutions of **1** in pH 7 water with NaCl electrolyte (0.1 M) exhibited a single irreversible reduction feature (SI Figure S5). The initial reduction features are assigned as $2e^-$ processes on the basis of previous reports and CPE experiments (vide infra).[7,8] The distinct behavior observed in chloride and in phosphate electrolytes indicates partial chloride displacement in phosphate buffer to form $[Cp^*Ir(bpy)(H_2O)]^{2+}$,[13] and $[Cp^*Ir(bpy)(H_2PO_4)]^+$,[14] as further evidenced by ^1H and $^{31}P\{^1H\}$ NMR studies that showed two minor species (<10% of total Ir) in D_2O containing ∼0.1 M pD 7 NaH_2PO_4/Na_2HPO_4. In pure D_2O, **1** was the only species observed.

Regardless of electrolyte, aqueous solutions of **1** show a second, quasi-reversible $1e^-$ reduction at −1.25 V (SI Figure S6). This feature is assigned to the $Ir^{III}-H^+/Ir^{II}-H$ couple of hydride **2**, suggesting that $2e^-$ reduction of **1** to form $Cp^*Ir^I(bpy)$ (**3**) is followed by rapid protonation.[7] Consistent with this assignment, the peak current at −1.25 V diminishes as the solution pH increases: as **3** becomes the dominant product upon reduction of **1**, the feature corresponding to the reduction of **2** disappears. Above pH 10, a new oxidation feature is also observed around −0.25 V, assigned as a $2e^-$ oxidation of **3**. At these high pH values, the voltammetric response is indicative of the neutral complex **3** adsorbing on the electrode (SI Figure S9). Similar adsorption is observed at pH < 10 when scanning beyond −1.3 V, at which point another neutral species, Cp*Ir(bpy)(H), is formed (SI Figure S6). Conditions in subsequent experiments were chosen to avoid such adsorption (see below for a discussion on homogeneity).

A stepwise electrolysis-photolysis experiment was undertaken to separately probe the role of electron transfer and photon absorption (Figure 3). Controlled potential electrolysis of **1** (λ_{max} = 340 nm (sh); ε_{340} = 2,800 M^{-1} cm^{-1}) was carried out protected from light and in pH 7 phosphate buffer. The product of dark electrolysis was confirmed to be hydride **2**, formed in high yield as judged by ^1H NMR spectroscopy (SI Figure S8) and UV−vis spectroscopy.[15] Electrochemically produced **2** exhibited an absorbance maximum (λ_{max} = 410 nm) and molar extinction coefficient (ε_{410} = 2400 M^{-1} cm^{-1}) similar to the authentic sample.[16] Cyclic voltammetry showed that the first reduction wave of **1** had also essentially disappeared, whereas the hydride redox couple remained. In a typical electrolysis with 2.5 mL of 1 mM **1**, the total charge passed during dark CPE was −433 mC (1.8 e^-/Ir), consistent with $2e^-$ reduction of **1** followed by protonation to form hydride **2**.

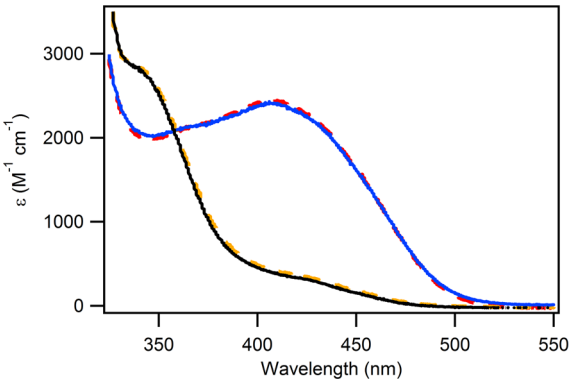

Figure 3. UV−vis spectra of 0.3 mM **1** in 0.1 M phosphate buffer (solid black), after 90 min of electrolysis at −0.9 V to form **2** (solid blue), and after 90 min of 460 nm photolysis to reform **1** (dashed orange). Subsequent electrolysis reformed **2** (dashed red) and photolysis reformed **1** (omitted for clarity). The molar extinction coefficient (ε) of each species was calculated assuming clean conversion (see text for details). Reticulated vitreous carbon working electrode, Pt wire counter electrode, Ag/AgCl (3 M NaCl) reference electrode.

Next, the same electrolysis solution containing in situ-generated hydride **2** was photolyzed. Whereas solutions of hydride **2** in neutral water are stable in the dark over several hours, irradiation with a 460 nm LED array leads to rapid consumption of **2**, as judged by UV−vis (Figure 3) and CV (SI Figure S10). Photolysis resulted in reformation of pale yellow **1**. Resubjecting the solution to CPE cleanly produced golden hydride **2**, which was again consumed upon photolysis, indicating stepwise catalysis. The evolved gas, confirmed to be H_2 by GC headspace analysis, was formed with 70% faradic efficiency. Faint orange luminescence was apparent to the naked eye during photolysis of concentrated solutions of **2**, suggesting the involvement of the previously reported excited state of $[Cp^*Ir(bpy)(H)]^+$, **2***, which has been reported to have an 80 ns lifetime at 298 K in MeCN.[17,18] Scheme 2 depicts a broad mechanism for photoelectrocatalytic H_2 evolution that is consistent with the stepwise studies. The detailed mechanism remains unclear at this time; the nature of the H_2 evolution step, in particular, could proceed via monometallic or bimetallic pathways and will be the focus of future mechanistic studies.

A slew of studies on the homogeneity of Cp*Ir-based catalysts compelled us to consider the possibility of Ir nanoparticle formation.[19] Three lines of evidence suggest that a molecular catalyst is likely to be responsible for the observed behavior. First, the stepwise electrolysis/photolysis study described above shows that the chloride complex **1** is electrochemically converted to the hydride complex **2** in high yield. If the electrochemical current was leading to deposition of nanoparticles or other decomposition, the yield of molecular species **2** should be low. Further, upon photolysis, H_2 gas and

dx.doi.org/10.1021/cs500441f | ACS Catal. 2014, 4, 2727−2733

Scheme 2. Proposed Intermediates in Photoelectrocatalytic Cycle

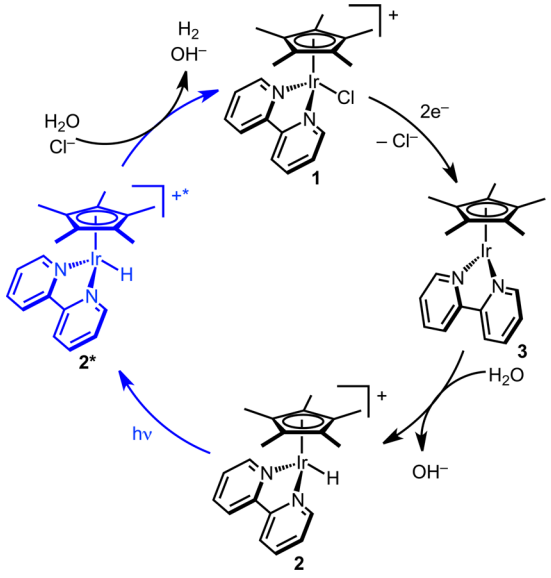

chloride **2** are formed in high yield; this cycle can be repeated three times without noticeable degradation (Figure 3). It is noteworthy that the study was monitored by optical spectroscopy, as IrO_x nanoparticles are highly colored; no absorption in the 600−800 nm range was observed. Second, a "rinse test" was performed: when the electrode was gently rinsed with water after a typical photoelectrocatalytic run and placed in a fresh phosphate solution containing no catalyst, the trace current that passed matched previous glassy carbon background scans (and showed no photoresponse). Finally, the kinetics of catalysis showed no induction period and controlled potential electrolyses maintained steady photocurrent for hours. These observations, along with the use of reductive, anaerobic conditions (as opposed to oxidizing, aerobic conditions under which Cp*Ir-based water oxidation catalysts decompose), suggest that catalyst degradation to nanoparticles is not a major factor.

Optimization of Photoelectrocatalytic Performance. Optimization of the photoelectrocatalytic hydrogen evolution reaction was carried out with the aid of kinetic studies. As discussed above, the initial rates were too slow for reliable data to be extracted from CV experiments. Reaction rate constants were therefore measured using chronoamperometry (CA). Although not commonly used to assess electrocatalysts, Delahay and Stiehl showed that CA data can provide an apparent rate constant for catalytic reactions.[20] The model assumes that electron transfer is fast, such that the observed rate constant is a reflection of a rate-determining chemical catalytic step (EC′ mechanism). Although the influence of light on the reaction may complicate such analysis, we have found CA convenient for obtaining an apparent rate constant, k_{obs}, for comparisons. Chronoamperometry of **1** was carried out at −1.0 V for 20 s both in the dark and under 460 nm illumination. Irradiated samples passed significantly more current than those protected from light (Figure 4A). The ratio of the light and dark currents was fit between 5 and 10 s to give k_{obs} = 0.037(9) s^{-1}. The observed rate constant varied linearly with light intensity (SI Figure S11), supporting the notion that photon fluence is a key parameter.

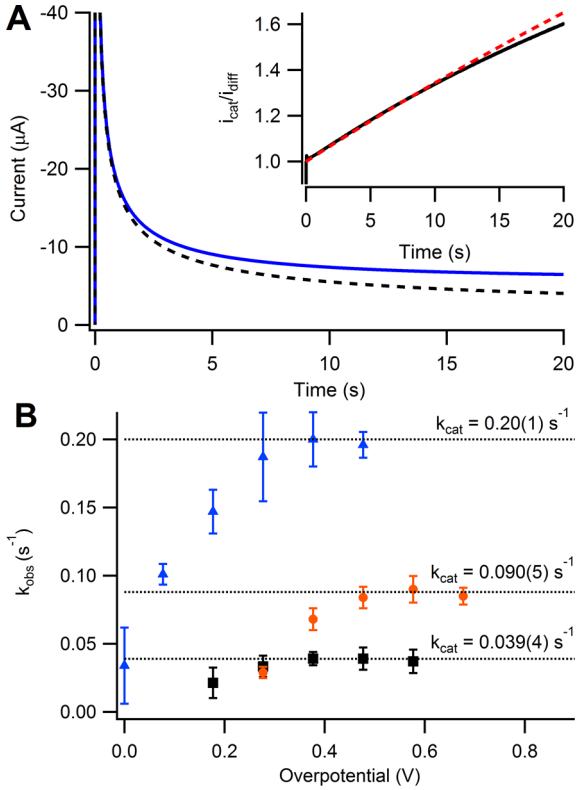

Figure 4. (A) Chronoamperometry of 1 mM **1** in pH 7 phosphate buffer in the dark (dashed black) and under 460 nm LED irradiation (solid blue) at −1 V vs NHE. Inset: ratio of the two CA traces (black) and fit (dashed red) with k_{obs} = 0.036 s^{-1}. (B) Apparent catalytic rate constants for **1** (black squares), **1-OMe$_2$** (orange circles), and **1-COOH$_2$** (blue triangles) as a function of potential. Error bars reflect two standard deviations in both directions as determined by between 3 and 7 experiments. Glassy carbon working electrode (3 mm disc), Pt wire counter electrode, Ag/AgCl (3 M NaCl) reference electrode.

The impact of potential on photoelectrocatalysis was investigated by varying the applied CA potential between −0.6 and −1.0 V (Figure 4B, black squares). The observed rate constant increased with increasing overpotential,[21] remaining steady with k_{obs} = 0.039(4) s^{-1} after −0.8 V. The catalytic onset potential is consistent with the notion that the key intermediate in H_2 evolution photoelectrocatalysis is the Ir^{III}−H^+ intermediate **2**, which is readily formed electrochemically at these potentials. Further reduction to the neutral Ir(II)−H is not required. A hydrogen evolution overpotential of only 190 mV (−0.60 V vs NHE at pH 7) is required to achieve half of the maximum catalytic rate, k_{obs} = 0.02(1) s^{-1};[21] this potential corresponds nicely to the relevant reduction wave of **1** (−0.61 V). In contrast, aqueous solutions of **1** *protected from light* do not show conclusive evidence of catalysis even upon subsequent reduction of **2** to the Ir^{II}−H intermediate. A related catalyst with pyrrole substituents, when electropolymerized onto an electrode surface, was reported to evolve H_2 via the Ir^{II}−H state under acidic conditions: pH 3 at −1.31 V, an approximate overpotential of 1.1 V.[8] When a photochemical step is harnessed, **1** catalyzes H_2 evolution at a more positive reduction potential and at neutral pH.

A variety of media were screened as supporting electrolytes for water reduction across a wide pH range. Sustained catalytic current over background was observed when 1 mM solutions of **1** in 0.1 M citrate buffer underwent CPE at −0.9 V (pH

dx.doi.org/10.1021/cs500441f | ACS Catal. 2014, 4, 2727−2733

adjusted to 4, 5, and 6 in separate experiments). A phosphate solution at pH 8 and borate buffer solutions at pH 9 and 10 also showed sustained CPE photocurrents (−1 V).

Facile tuning by ligand substitution is a key feature of many molecular catalysts, and indeed, the photoelectrocatalytic H_2 evolution behavior is not unique to complex **1**. A large variety of substituted bipyridine analogues are known, and complexes of a few of these were screened in initial studies. Sustained currents over 1 h were observed when electrochemical cells containing solutions of [Cp*Ir(bpy-OMe)(Cl)][Cl] (**1-OMe$_2$**) and [Cp*Ir(bpy-COOH)(Cl)][Cl] (**1-COOH$_2$**) (bpy-X = 4,4′-X-2,2′-bipyridine, X = OMe, COOH) were held at −1.0 V and irradiated with a 460 nm LED in pH 7 phosphate buffer.

Surprisingly, the observed rate constants obtained from chronoamperometry did not follow the trends expected for electrocatalysts. The catalyst reduced at the most negative potential, **1-OMe$_2$**, gave k_{obs} = 0.090(5) s^{-1} at −1 V, whereas the catalyst reduced at the most positive potential, **1-COOH$_2$** (deprotonated under the experimental conditions), was the top performer, with k_{obs} = 0.20(1) s^{-1} at −0.8 V (Figure 4B). Carboxylate-substituted catalyst **1-COOH$_2$** also operates at lower overpotentials than **1**, and CV traces show the onset of catalysis occurs *just prior to* the thermodynamically required potential for H_2 evolution (Figure 5), with k_{obs} = 0.034 s^{-1} at 0

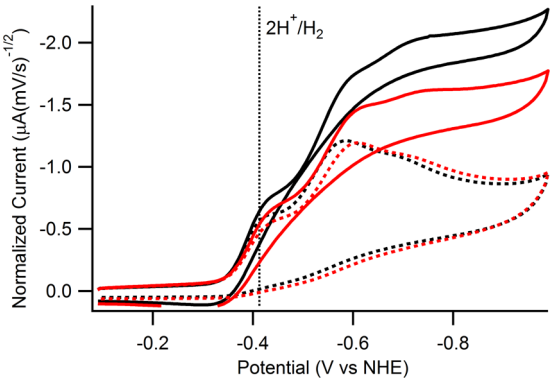

Figure 5. CV of 1 mM **1-COOH$_2$** in 0.1 M phosphate buffer (pH 7) at 25 mV·s^{-1} under 460 nm LED light (solid black) and dark (dashed black) and at 50 mV·s^{-1} in the light (solid red) and dark (dashed red). Glassy carbon working electrode (3 mm disc), Pt wire counter electrode, Ag/AgCl (3 M NaCl) reference electrode. Current is scan-rate-normalized: normalized current of diffusion-controlled processes is constant with changing scan rate while normalized current of catalytic waves increases as scan rate decreases.

V overpotential. This situation is possible only when photon energy is being utilized and suggests that further catalyst optimization may lead to significant energy storage.

It is remarkable that **1-COOH$_2$** is both the fastest catalyst and features the lowest overpotential, in light of the general trend for molecular electrocatalysts that higher overpotentials will give higher reactivity. Inspection of the absorption spectra reveals that [Cp*Ir(bpy-COOH)(H)]$^+$ has excellent overlap with the 460 nm LED lamp used in these studies (Figure 6). This presumably leads to an increased external quantum efficiency, perhaps explaining the superior photoelectrochemical performance of **1-COOH$_2$** at low overpotential.

CONCLUSIONS

A novel approach to H_2 evolution using molecular photoelectrocatalysts has been introduced. A single molecular catalyst

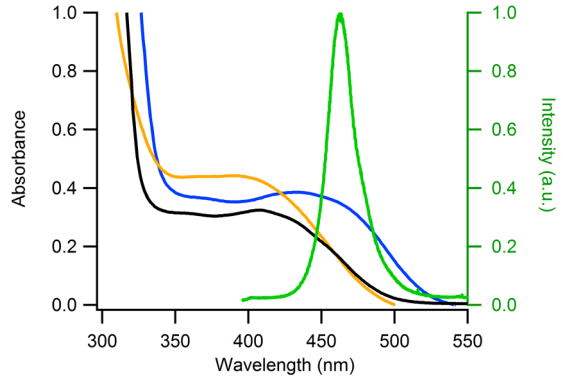

Figure 6. Absorption spectra of electrochemically generated [Cp*Ir(bpy)(H)]$^+$ (black), [Cp*Ir(bpy-OMe)(H)]$^+$ (orange), and [Cp*Ir(bpy-COOH)(H)]$^+$ (blue) in 0.1 M phosphate buffer (pH 7) with the spectrum of the 460 nm LED lamp (green).

undergoes electrochemical hydride formation, followed by photochemical H_2 release. Water reduction is facilitated by three different Ir catalysts and visible light over a wide pH range at low overpotentials. Hydrogen evolution at the thermodynamic potential was observed, with rate constants of ∼0.1 s^{-1} at ∼100 mV electrochemical overpotential.

Combining aspects of photocatalysis and electrocatalysis leads to a number of interesting observations. In comparison with typical hydrogen evolution electrocatalysts, visible light excitation leads to a dramatic reduction in electrochemical applied overpotential, as the required energy comes from light instead of electricity. Further, electrocatalysts typically feature trade-offs between the required potential for catalytic onset and catalytic activity. By incorporating a photochemical step, this linear correlation is broken, and the more easily reduced catalyst **1-COOH$_2$** also was found to be the most active because of better photon absorption ability. In comparison with typical photocatalysts, the use of an electrode lifts the requirement for sacrificial reducants. Whereas a complex mixture of light absorbers, redox mediators, catalysts, and sacrificial reagents are often required for photocatalytic H_2 evolution, the present system features a single component that acts as light absorber and catalyst.

On the basis of the approach presented here, further improvements can be envisioned: for example, the 460 nm (2.6 eV) lamp provides substantial excess photon energy that is currently not fully utilized. Future work will focus on elucidating the detailed mechanism of the reaction and developing new catalysts capable of sustaining faster hydrogen evolution rates, even while absorbing lower energy light.

EXPERIMENTAL SECTION

General Considerations. Procedures were carried out under nitrogen except where noted. 2,2′-Bipyridine (bpy) and 4-4′-dimethoxy-2-2′-bipyridine (bpy-OMe), 4,4′-carboxyl-2,2′-bipyridine (bpy-COOH), sodium hydroxide, phosphoric acid, and pentamethylcyclopentadiene (Cp*H) were obtained from either Alfa Aesar or Sigma-Aldrich. Sodium phosphate monobasic hydrate was obtained from Mallinckrodt. $IrCl_3 \cdot 3H_2O$ was obtained from J&J Materials Inc. Commercial HPLC-grade water was used as a solvent. Deuterium oxide was purchased from Cambridge Isotope Laboratories, Inc. Electrochemical experiments were performed on a Pine WaveNow potentiostat or Pine WaveDriver bipotentiostat controlled by Aftermath software. Details on specific electrochemical experi-

dx.doi.org/10.1021/cs500441f | ACS Catal. 2014, 4, 2727−2733

ments are described below. Solution pH was recorded using an OrionStar A111 pH meter with a Beckman-Coulter pH probe. UV−vis spectra were obtained using an Agilent Cary 60 spectrophotometer or an Ocean Optics USB2000+ spectrometer with a DT-MINI-2GS deuterium and tungsten halogen light source controlled by OceanView software.

A Varian 450-GC with a pulsed discharge helium ionization detector was used to quantify H_2. A calibration curve was constructed from samples of 0.5, 1.0, 3.0, and 5.0 v/v % H_2 in air. All gas transfers were performed with a 1.0 or 10 mL Vici Pressure-Lok Precision Analytical Syringe. As much as possible, septa were pierced only once. NMR spectra were obtained on 400 or 600 MHz spectrometers. ^{1}H NMR spectra were referenced to the residual solvent signals (or with acetone or sodium tosylate as an internal standard in D_2O).[22] Spectra were processed using the MestReNova software suite from Mestrelab Research S. L. The solution acidity in NMR experiments is reported as pD, obtained by addition of +0.4 to the reading of a pH electrode that was calibrated using H_2O standards.[23]

Synthesis. The catalysts [Cp*Ir(bpy)(Cl)][Cl],[9] [Cp*Ir(bpy-OMe)(Cl)][Cl],[9] [Cp*Ir(bpy-COOH)(Cl)][Cl],[6c] and $[Cp^*Ir(Cl)_2]_2$[24] were prepared according to literature procedures. The hydride [Cp*Ir(bpy)(H)][OTf] was synthesized by a modified literature procedure:[25] the PF_6^- salt of the starting aquo was replaced with the corresponding triflate salt, $[Cp^*Ir(bpy)(H_2O)][OTf]_2$;[26] after stirring in a 3 M formate solution (pH 5) for 2 h at 298 K, extraction with CH_2Cl_2 followed by removal of solvents under vacuum gave pure **2**. Catalyst identity and purity (>99%) was established by ^{1}H NMR spectroscopy. The spectroscopic features closely matched the published data.

Photochemistry. Photolysis was conducted using a 500 lm blue LED lamp from EagleLight. The wavelength of maximum intensity was 460 nm (±12 nm at half-max intensity), as measured with an Ocean Optics USB2000+ controlled by Overture software (Figure 6). In the power dependence experiment, a 460 nm (±21 nm at half-max intensity) dimmable LED light strip from Super Bright LEDs was used. An estimate of the external quantum efficiency was obtained by measuring photon flux with a Coherent LM-2VIS photodiode in conjunction with a Coherent FieldMax$_{II}$ Laser Power/Energy Meter. The photodiode was positioned at the same distance from the lamp as the electrode, and a piece of curved glass was used to approximate the conditions of the cell. Photon flux was measured to be 1.76×10^{-8} mol photons·s^{-1} in the 0.54 cm^2 area of the electrode.

Electrochemistry. Unless otherwise noted, all electrochemical experiments were performed in a divided H-cell with a three-electrode configuration (SI Figure S22). A carbon working electrode (specific material varied with experiment, see below) and platinum wire counter electrode were positioned on either side of the fine frit. A Ag/AgCl (3 M NaCl) reference electrode was placed in the counter electrode compartment in a small glass tube fitted with a Vycor. Solutions were made by adjusting the pH of solutions of the appropriate concentration of sodium phosphate monobasic with NaOH and were thoroughly degassed by sparging with nitrogen for at least 15 min before beginning an experiment. All potentials are reported relative to NHE, with values obtained by adding 0.21 V to the experimentally observed potential vs Ag/AgCl.[27] Overpotentials (to achieve a certain catalytic efficiency) were calculated by subtracting the formal potential for H_2 evolution ($E^\circ_{H+/H2}$ = 0−0.059·pH) from the applied potential at which catalysis was experimentally observed.[28]

Cyclic voltammetry experiments were carried out with a 3-mm-diameter glassy carbon disc working electrode (polished with 0.05 μm alumina powder between scans). For experiments under irradiation, the 460 nm LED lamp was placed directly below the glassy carbon electrode at a fixed distance (SI Figures S23 and S24).

Controlled potential electrolysis experiments were carried out with reticulated vitreous carbon (RVC) impaled on a graphite rod wrapped in copper wire (above the water line) as the working electrode. In the illuminated experiments, a 460 nm lamp was placed approximatly 1 inch away from the cell. In the dark experiments, the cell was wrapped in aluminum foil. In the shutter experiment, the light was turned on and off periodically; the cell was not wrapped in aluminum foil during the dark stages. For a diagram of experimental setup, see SI Figures S25 and S26.

Faradic efficiency was determined by monitoring the pH change over the course of a CPE experiment. A solution of 1 mM [Cp*Ir(bpy)(Cl)][Cl] in 50 mM phosphate was held at −0.9 V while being irradiated with 460 nm LED light for 90 min, with the pH probe inserted into the working electrode compartment of the H-cell. For each molecule of H_2 formed, two OH^- ions are produced. The amount of hydroxide corresponding to the observed pH change was determined by titration of an identical sample with 0.1 M NaOH.[11] A control experiment, in which a pH 7 phosphate buffer with no catalyst was held at −0.9 V, showed minimal charge accumulation. Whereas the solution pH changed by 1.0 unit when the catalyst was present, without catalyst, the pH changed by <0.1 unit, suggesting little or no H_2 production at the electrode under the standard photoelectrolysis conditions.

Headspace detection of H_2 by gas chromatograph was performed in the same cell that was used for CV and CPE experiments. Every effort was made to configure the cell such that any leaks were minimized. After CPE at −0.9 V for 30 min, a headspace sample was obtained before and after photolysis using a gastight 1.0 mL syringe. The volume % hydrogen was quantified by comparison to a calibration curve. Before photolysis, no H_2 peak was observed by GC. After photolysis, a prominent H_2 peak was observed in the GC trace. Integration and comparison with the calibration curve established a 70% faradic efficiency.

To show stepwise catalysis by UV−vis (Figure 3), a 200 mL capacity divided cell was used. The Pt wire was positioned in 3 mL in 0.1 M pH 7 phosphate buffer across a frit from the RVC working electrode and Ag/AgCl reference electrode. A 0.3 mM solution of **1** (40 mL 0.1 M pH 7 phosphate buffer) was added to the working electrode chamber and degassed. UV−vis were obtained by syringing 3 mL of solution into septa-capped cuvettes under N_2. The samples were returned to the cell after the spectra were taken. Spectra were collected at five points: initially, after exhaustive electrolysis at −0.9 V, after exhaustive photolysis, after a second electrolysis, and after a final photolysis.

Chronoamperometry was carried out in the standard H-cell, electrode configuration, and lamp positioning described above for CV. The potential was held between −0.4 and −1.1 V, based on the location of the reduction wave observed by cyclic voltammetry. At each potential, two traces were obtained in the light and in that dark with electrode polishing between each

experiment. The ratio of the current in the light (i_{cat}) to the current in the dark (i_{diff}) was fit to the following equation:

$$\frac{i_{cat}}{i_{diff}} = (k_{obs}t)^{1/2}\left[\pi^{1/2}\mathrm{erf}((k_{obs}t)^{1/2}) + \frac{\exp(-k_{obs}t)}{(k_{obs}t)^{1/2}}\right]$$

where k_{obs} is the rate constant for the turnover-limiting chemical step and t is time.[20] The data was least-squares-fit between 5 and 10 s using the Excel solver function. In the regime of fast electron transfer at high applied potentials, k_{obs} reaches a limiting plateau, k_{cat}, the apparent rate constant of the chemical steps. Though deviations from k_{cat} are suggestive of mechanistic complexity, the CA traces at low applied potentials are still indicative of catalysis.

A control reaction to test whether adsorbed species might be the true catalyst was performed as follows: a standard CA experiment was carried out at −0.9 V in phosphate buffer, followed by gently rinsing the carbon electrode with water and repeating the CA experiment in a fresh phosphate buffer solution containing no catalyst. When moved to a fresh electrolyte solution containing no catalyst, no current over background was observed in the CA experiment, and no current enhancement under photolysis was observed, suggesting that catalyst adsorption is not a factor in this system.

■ ASSOCIATED CONTENT

Supporting Information

Additional figures, schematics and photographs of photoelectrochemical cells. This material is available free of charge via the Internet at http://pubs.acs.org/.

■ AUTHOR INFORMATION

Corresponding Author

*E-mail: ajmm@email.unc.edu.

Notes

The authors declare no competing financial interest.

■ ACKNOWLEDGMENTS

The authors gratefully acknowledge funding from the University of North Carolina at Chapel Hill and the Royster Society of Fellows (C.L.P.). Preliminary studies on Ir hydrides were supported by the NSF Center for Enabling New Technologies through Catalysis (CENTC), CHE-1205189. This research made use of instrumentation funded by the UNC EFRC: Center for Solar Fuels, an Energy Frontier Research Center supported by the U.S. Department of Energy, Office of Science, Office of Basic Energy Sciences, under Award No. DE-SC0001011.

■ REFERENCES

(1) (a) Esswein, A. J.; Nocera, D. G. *Chem. Rev.* **2007**, *107*, 4022−4047. (b) Teets, T. S.; Nocera, D. G. *Chem. Commun.* **2011**, *47*, 9268−9274. (c) Berardi, S.; Drouet, S.; Francàs, L.; Gimbert-Suriñach, C.; Guttentag, M.; Richmond, C.; Stoll, T.; Llobet, A. *Chem. Soc. Rev.* **2014**, DOI: 10.1039/C3CS60405E. (d) Dempsey, J. L.; Winkler, J. R.; Gray, H. B. In *Comprehensive Inorganic Chemistry II: From Elements to Applications*; Reedjik, J., Poeppelmeier, K., Eds.; Elsevier: Oxford, 2013; Vol. 8, p 553−565.

(2) Thoi, V. S.; Sun, Y.; Long, J. R.; Chang, C. J. *Chem. Soc. Rev.* **2013**, *42*, 2388−2400.

(3) Eckenhoff, W. T.; Eisenberg, R. *Dalton Trans.* **2012**, *41*, 13004−13021.

(4) Osterloh, F. E. *Chem. Soc. Rev.* **2013**, *42*, 2294−2320.

(5) (a) Kalyanasundaram, K.; Grätzel, M. *Photochem. Photobiol.* **1984**, *40*, 807−822. (b) Otruba, J. P.; Neyhart, G. A.; Dressick, W. J.; Marshall, J. L.; Sullivan, B. P.; Watkins, P. A.; Meyer, T. J. *J. Photochem.* **1986**, *35*, 133−153. (c) Deronzier, A.; Essakalli, M. *J. Chem. Soc., Chem. Commun.* **1990**, 242−244.

(6) (a) Ziessel, R. *J. Chem. Soc., Chem. Commun.* **1988**, 16−17. (b) Ziessel, R. *Angew. Chem., Int. Ed.* **1991**, *30*, 844−847. (c) Ziessel, R. *J. Am. Chem. Soc.* **1993**, *115*, 118−127.

(7) Steckhan, E.; Herrmann, S.; Ruppert, R.; Dietz, E.; Frede, M.; Spika, E. *Organometallics* **1991**, *10*, 1568−1577.

(8) Caix, C.; Chardon-Noblat, S.; Deronzier, A.; Ziessel, R. *J. Electroanal. Chem.* **1993**, *362*, 301−304.

(9) Dadci, L.; Elias, H.; Frey, U.; Hornig, A.; Koelle, U.; Merbach, A. E.; Paulus, H.; Schneider, J. S. *Inorg. Chem.* **1995**, *34*, 306−315.

(10) Costentin, C.; Robert, M.; Savéant, J.-M. *Chem. Soc. Rev.* **2013**, *42*, 2423−2436.

(11) Karunadasa, H. I.; Montalvo, E.; Sun, Y.; Majda, M.; Long, J. R.; Chang, C. J. *Science* **2012**, *335*, 698−702.

(12) Low TON values are a result of low catalyst concentrations near the surface of the electrode. The TON values confirm that every Ir complex turns over at least once, but are not useful as a measure of catalyst activity or longevity.

(13) The pK_a of $[Cp^*Ir(bpy)(H_2O)]^{2+}$ has been reported as 6.6 (Ogo, S.; Makihara, N.; Watanabe, Y. *Organometallics* **1999**, *18*, 5470−5474) and 7.5 (ref 9).

(14) A few Ir(III) phosphate complexes have been reported. For example, see: (a) Hendry, P.; Sargeson, A. M. *J. Am. Chem. Soc.* **1989**, *111*, 2521−2527. (b) Hendry, P.; Sargeson, A. M. *Inorg. Chem.* **1990**, *29*, 97−104. (c) Li, C.; Wang, C.; Villa-Marcos, B.; Xiao, J. *J. Am. Chem. Soc.* **2008**, *130*, 14450−14451.

(15) (a) Ladwig, M.; Kaim, W. *J. Organomet. Chem.* **1992**, *439*, 79−90. (b) Youinou, M.-T.; Ziessel, R. *J. Organomet. Chem.* **1989**, *363*, 197−208.

(16) The isolated sample of $[Cp^*Ir(bpy)(H)][OTf]$ had $\varepsilon_{410} = 2100$ M^{-1} cm^{-1}. The extinction coefficients of **2** should be taken as approximate values because of the light- and air-sensitive nature of the hydride. The triflate salt also has limited water solubility.

(17) Sandrini, D.; Maestri, M.; Ziessel, R. *Inorg. Chim. Acta* **1989**, *163*, 177−180.

(18) Suenobu, T.; Guldi, D. M.; Ogo, S.; Fukuzumi, S. *Angew. Chem., Int. Ed.* **2003**, *42*, 5492−5495.

(19) (a) Crabtree, R. H. *Chem. Rev.* **2012**, *112*, 1536−1554. (b) Limburg, B.; Bouwman, E.; Bonnet, S. *Coord. Chem. Rev.* **2012**, *256*, 1451−1467. (c) Artero, V.; Fontecave, M. *Chem. Soc. Rev.* **2013**, *42*, 2338−2356.

(20) (a) Delahay, P.; Stiehl, G. L. *J. Am. Chem. Soc.* **1952**, *74*, 3500−3505. (b) Bard, A. J.; Faulkner, L. R. *Electrochemical Methods: Fundamentals and Applications*; Wiley: New York, 2000.

(21) Overpotential is defined according to page 7 of ref 20b, "The additional potential (beyond the thermodynamic requirement) needed to drive a reaction at a certain rate is called the *overpotential*." The overpotentials cited in the text correspond to the specific overpotential recommended for homogeneous catalysts. See: Appel, A. M.; Helm, M. L. *ACS Catal.* **2014**, *4*, 630−633.

(22) Fulmer, G. R.; Miller, A. J. M.; Sherden, N. H.; Gottlieb, H. E.; Nudelman, A.; Stoltz, B. M.; Bercaw, J. E.; Goldberg, K. I. *Organometallics* **2010**, *29*, 2176−2179.

(23) Glasoe, P. K.; Long, F. A. *J. Phys. Chem.* **1960**, *64*, 188−190.

(24) White, C.; Yates, A.; Maitlis, P. M. *Inorg. Synth.* **1992**, *29*, 228−230.

(25) Abura, T.; Ogo, S.; Watanabe, Y.; Fukuzumi, S. *J. Am. Chem. Soc.* **2003**, *125*, 4149−4154.

(26) Miller, A. J. M.; Heinekey, D. M.; Mayer, J. M.; Goldberg, K. I. *Angew. Chem., Int. Ed.* **2013**, *52*, 3981−3984.

(27) Smith, T. J.; Stevenson, K. J. In *Handbook of Electrochemistry*; Zoski, C. G., Ed.; Elsevier: Amsterdam. 2007; p 75.

(28) Walter, M. G.; Warren, E. L.; McKone, J. R.; Boettcher, S. W.; Mi, Q.; Santori, E. A.; Lewis, N. S. *Chem. Rev.* **2010**, *110*, 6446−6473.